JACC: BASIC TO TRANSLATIONAL SCIENCE VOL. 4, NO. 1, 2019

MINI FOCUS ON SGLT2 INHIBITORS

Empagliflozin Improves Diastolic Function in a Nondiabetic Rodent Model of Heart Failure With Preserved Ejection Fraction

Kim A. Connelly, MBBS, PhD, Yanling Zhang, MD, Aylin Visram, BSc, Andrew Advani, BSc, MBChB, PhD, Sri N. Batchu, PhD, Jean-François Desjardins, MSc, Kerri Thai, BSc, Richard E. Gilbert, MBBS, PhD

VISUAL ABSTRACT

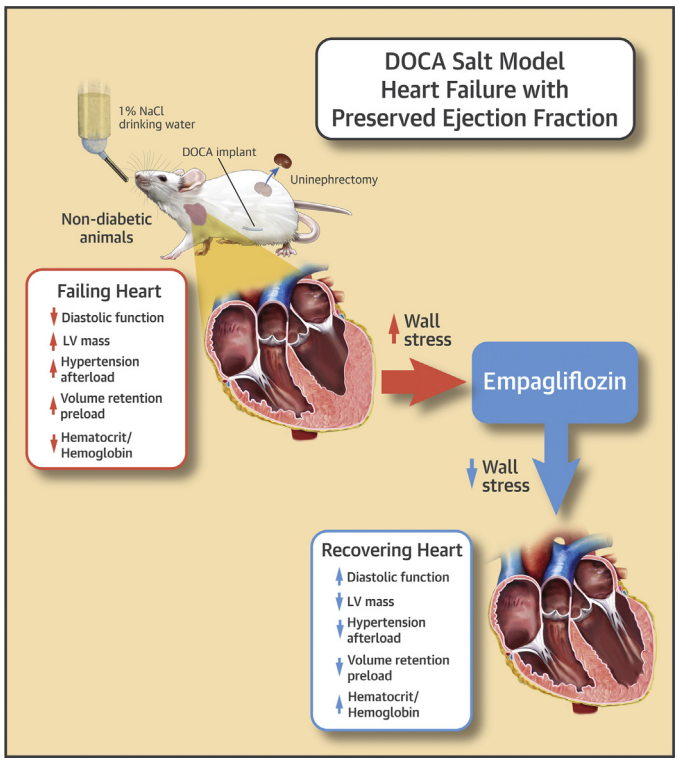

Connelly, K.A. et al. J Am Coll Cardiol Basic Trans Science. 2019;4(1):27–37.

HIGHLIGHTS

- This study evaluated the impact of the sodium-glucose–linked co-transporter-2 inhibitor, empagliflozin, on cardiac function and structure in a nondiabetic model of heart failure with preserved ejection fraction in the deoxycorticosterone acetate salt-sensitive rat.
- Deoxycorticosterone acetate rats developed hypertension, left ventricular hypertrophy, and diastolic dysfunction as measured by the time constant of relaxation, Tau.
- Empagliflozin therapy, which did not significantly reduce blood pressure, increased hematocrit, reduced left ventricular and cardiomyocyte hypertrophy, and reduced wall stress, which led to improved diastolic function (shortening of Tau).
- Empagliflozin treatment did not modify molecular markers of metabolism or hypertrophy, nor did it significantly affect key proteins involved in myocardial calcium handling.
- This study concluded that the sodium-glucose–linked co-transporter-2 inhibitor, empagliflozin, in a nondiabetic model of heart failure with preserved ejection fraction improved cardiac diastolic function and reduced wall stress primary through a reduction in cardiac preload, and also altered hemodynamics.

ISSN 2452-302X https://doi.org/10.1016/j.jacbts.2018.11.010

JACC: BASIC TO TRANSLATIONAL SCIENCE VOL. 4, NO. 1, 2019
FEBRUARY 2019:27–37

ABBREVIATIONS AND ACRONYMS

ANP = atrial natriuretic peptide

DOCA = deoxycorticosterone acetate

GADPH = glyceraldehyde 3-phosphate dehydrogenase

HF = heart failure

HFpEF = heart failure with preserved ejection fraction

HFrEF = heart failure with reduced ejection fraction

LV = left ventricular

SGLT2i = sodium-glucose–linked co-transporter-2 inhibitor

UNX = uninephrectomy

SUMMARY

Recent studies send an unambiguous signal that the class of agents known as sodium-glucose–linked co-transporter-2 inhibitors (SGLT2i) prevent heart failure hospitalization in patients with type 2 diabetes. However, the mechanisms remain unclear. Herein the authors utilize a rodent model of heart failure with preserved ejection fraction (HFpEF), and demonstrate that treatment with the SGLT2i empagliflozin, reduces left ventricular mass, improving both wall stress and diastolic function. These findings extend the observation that the main mechanism of action of empagliflozin involves improved hemodynamics (i.e., reduction in preload and afterload) and provide a rationale for upcoming trials in patients with HFpEF irrespective of glycemic status. (J Am Coll Cardiol Basic Trans Science 2019;4:27–37)

Despite significant advances in cardiovascular diagnostics and therapeutics, heart failure (HF) remains a common condition with significant morbidity and considerable mortality; regardless of underlying etiology, approximately 25% of those hospitalized will die (1). Although there have been major advances with multiple therapeutic agents of proven benefit in HF with reduced ejection fraction (HFrEF), heart failure with preserved ejection fraction (HFpEF) lacks evidence-based therapies (2).

SEE PAGE 38

Sodium-glucose–linked co-transporter-2 inhibitors (SGLT2is) increase urinary glucose excretion off-loading energy, lower plasma glucose and reduce body weight, as well as inducing modest diuresis that assists in blood pressure reduction. In addition to its antihyperglycemic actions, recent cardiovascular outcome studies have demonstrated a reduction in HF hospitalizations (3,4). Although the importance of these trials cannot be overstated, their outcomes are mostly unexpected. It is uncertain whether this drug class may provide similar benefit in both HFpEF and HFrEF or in only 1 of these conditions. Moreover, the magnitude of the effect of this therapy on HF hospitalization and the rapidity of its onset suggest that the cardioprotective properties of SGLT2is are greater than their ability to lower glucose. These findings have led not only to speculation as to how this antihyperglycemic drug class might exert its salutary effects but have also led to consideration that they may be also effective in the nondiabetic setting.

Recognizing the limited cardiac function data available from the aforementioned cardiovascular outcome trials in diabetes and the unmet clinical need in treating HFpEF, we sought to determine the effects of SGLT2 inhibition in HFpEF in the nondiabetic setting using a well-established animal model of the disease.

METHODS

ANIMALS. Experiments were conducted in 8-week old male Sprague-Dawley rats according to standard protocol for the deoxycorticosterone acetate (DOCA) hypertensive salt model, in which implants were prepared by mixing 200 mg of mineralocorticoid in

From the Keenan Research Centre, Li Ka Shying Knowledge Institute, St. Michael's Hospital, Toronto, Ontario, Canada. This study was supported by research grants from the St. Michael's Hospital Foundation, an investigator-initiated grant from Boehringer Ingelheim, as well as from the Canada Research Chair program (awarded to Dr. Gilbert). Dr. Connelly is supported by a new investigator reward from the CIHR and an early researcher award from the Ministry of Ontario. Dr. Advani is supported by a Diabetes Investigator Award from Diabetes Canada. Drs. Connelly, Advani, and Gilbert are listed as inventors on a patent application by Boehringer Ingelheim on the use of DPP-4 inhibitors in heart failure. Dr. Connelly has received research grants from AstraZeneca and Boehringer Ingelheim; has received travel support from Boehringer Ingelheim; and has received honoraria for speaking engagements and ad hoc participation in advisory boards from AstraZeneca, Boehringer Ingelheim, Sevier, Merck, Novo Nordisk, and Janssen. Dr. Advani has received research support from AstraZeneca and Boehringer Ingelheim. Dr. Gilbert is a shareholder in Certa, OccuRx, and Fibrocor Therapeutics; has received research grants from AstraZeneca and Boehringer Ingelheim; has received travel support from AstraZeneca; and has received honoraria for speaking engagements and ad hoc participation in advisory boards from AstraZeneca, Boehringer Ingelheim, and Janssen. All other authors have reported that they have no relationships relevant to the contents of this paper to disclose.

All authors attest they are in compliance with human studies committees and animal welfare regulations of the authors' institutions and Food and Drug Administration guidelines, including patient consent where appropriate. For more information, visit the *JACC: Basic to Translational Science* author instructions page.

Manuscript received May 1, 2018; revised manuscript received November 13, 2018, accepted November 14, 2018.

silicone rubber (5). Implanted rats then received 1% sodium chloride as drinking water, whereas uninephrectomy (UNX) rats were given tap water. One week later, rats were randomized to receive either empagliflozin mixed in chow (0.35 mg/g, gift of Boehringer Ingelheim, Ingelheim, Germany) or a control diet that coincided with DOCA implantation.

Four weeks after DOCA implantation, rats underwent echocardiography and cardiac catheterization. All procedures were performed in the research vivarium under anesthesia using 2.5% isoflurane. Systolic blood pressure was measured in conscious animals using an occlusive tail-cuff plethysmograph (Powerlab, ADInstruments, Colorado Springs, Colorado) (6). Before the animals were killed, they were housed in metabolic cages, and 24-h urine collections were obtained for measurement of glucose, sodium, and ß-OH butyrate excretion. Animals then underwent echocardiography and cardiac catheterization as described in the following. After these procedures, animals were killed, and their hearts were harvested for structural and molecular measurements. Tibial length was measured to provide a morphometric index for cardiac hypertrophy and lung weight (7). All animals were housed with 2 per cage at the St. Michael's Hospital Animal Research Vivarium in a temperature-controlled (22°C) room with a 12-h light/dark cycle and ad libitum access to commercial standard rat chow.

All animal studies were approved by the St. Michael's Hospital Animal Care Committee in accordance with the Guide for the Care and Use of Laboratory Animals (National Institute of Health Publication No. 85-23, revised 1996).

ECHOCARDIOGRAPHY. Transthoracic echocardiography was performed, as previously described (8), under light anesthesia (1% isoflurane supplemented with 100% oxygen) before the animals were killed. Images were acquired using a high-frequency ultrasound system (Vevo 2100, MS-250 transducer, Visualsonics, Toronto, Ontario, Canada). Two-dimensional, long-axis images of the left ventricle (LV) in parasternal long- and short-axis views with M-mode measurements at mid-papillary muscle level and linear dimensions were analyzed offline (Vevo 2100 software, version 1.8) using the standard leading edge-to-leading edge technique by a single investigator, who was blinded to treatment. The percentage of fractional shortening (FS%) was calculated according to the formula: FS% = (LVIDd - LVIDs)/LVIDd × 100, where LVIDd and LVIDs are end-diastolic diameter and end-systolic diameter, respectively, as previously described. LV wall stress (σ) was calculated by the equation: $\sigma = PR_i/2h(1 + h/2R_i)$, where P = systolic pressure, R_i = LV inner diameter (LVID), and h = LV wall thickness (9). Three consecutive cardiac cycles were averaged for all analyses.

CARDIAC CATHETERIZATION. Cardiac catheterization was performed as previously published (6). Briefly, rats were anesthetized with 2% isoflurane, intubated using a 14-gauge catheter, and ventilated using a pressure-controlled ventilator (TOPO ventilator, Kent Scientific, Torrington, Connecticut). Adequacy of anesthesia was assessed by lack of response to surgical manipulation and loss of muscular tone. Rats were placed in the supine position on a water circulating heating pad and a 2-F pressure–volume catheter (SPR-838, Millar Instruments, Inc., Houston, Texas) was inserted into the right carotid artery and advanced into the LV, and pressure–volume loops were generated. All pressure–volume loops were obtained with the ventilator turned off for 5 to 10 s and the animal apneic.

Data were acquired and recorded with a MPVS ultra data acquisition system (Millar Instruments) and LabChart Pro software (CHART 8.1 ADInstruments Inc., Colorado Springs, Colorado) under steady-state conditions and following inferior vena cava occlusion (pre-load reduction). Conductance signals acquired with the Millar catheter were calibrated with the estimated LV volumes derived from echocardiography by using a 2-point calibration method, and matching LV maximal and minimal conductance signals and end-diastolic and end-systolic volume were measured in the long-axis view. Using the pressure conductance data, functional parameters were then calculated, as previously reported (10).

HISTOPATHOLOGY. The extent of cardiac myocyte hypertrophy was determined on hematoxylin and eosin–stained sections, as previously reported (7). In brief, stained sections were scanned digitally by high resolution microscopy (Ultra-Resolution Digital Scanning System, Aperio Technologies Inc., Vista, California), and images were analyzed with NDP view2 software (Hamamatsu Photonics, Hamamatsu City, Japan). Cardiac myocytes with elliptical nuclei in the transverse section were selected. Diameter measurements were taken membrane-to-membrane across the narrowest point crossing the nucleus. The average diameter of 30 to 50 myocytes per animal was measured, as previously described (11).

WESTERN BLOTTING. For preparation of cytosolic fraction, heart tissues were minced and homogenized in homogenization buffer containing sucrose (250 mM), Tris-hydrogen chloride (10 mM),

TABLE 1 Animal Characteristics

	UNX + Control	UNX + Empa	DOCA + Control	DOCA + Empa
Body weight (g)	542 ± 25	490 ± 13*	423 ± 13	352 ± 9*†
LV weight/TL (mg/mm)	22 ± 1	20 ± 0	31 ± 1*	25 ± 1†
LW/TL (mg/mm)	39 ± 1	37 ± 1	44 ± 1*	38 ± 1†
Right kidney weight/TL (mg)	51 ± 1	62 ± 1*	104 ± 5*	90 ± 3*†
Food intake (g/24 h)	32 ± 2	31 ± 1	26 ± 2*	25 ± 1*
Water intake (ml/24 h)	19 ± 5	42 ± 4*	151 ± 14*	228 ± 25*†
Urine volume (ml/24 h)	28 ± 4	49 ± 5*	150 ± 13*	219 ± 24*†

Values are mean ± SEM. n = 7 to 8 in uninephrectomy (UNX) control and UNX empagliflozin (Empa) groups; n = 16 and 15 in deoxycorticosterone acetate (DOCA) control and Emp groups, respectively. *p < 0.05 versus UNX control group. †p < 0.05 versus DOCA control group.

LV weight/TL = left ventricular weight/tibial length; LW/TL = lung weight/tibial length ratio.

ethylenediaminetetraacetic acid (1 mM), sodium orthovanadate (1 mM), sodium flouride (1 mM), and a protease inhibitor cocktail (12). Immunoblotting of heart homogenates was performed on nitrocellulose membranes with antibodies in the following concentrations: phosphorylated phospholamban (phospho-PLN, Ser16) 1:1,000 (A285); Sarcoplasmic reticulum uptake Ca2+-ATPAase (SERCA2a) 1:1,000 (IID8F6); phospho-PLN (Thr17) 1:1,000 (#sc-17024, Santa Cruz Biotechnology, Dallas, Texas), phosphorylated Ca2+/calmodulin-dependent protein kinase II (CAMKII) 1:1000 (#sc-32289, Santa Cruz Biotechnology), total CAMKII 1:1000 (#sc-5306, Santa Cruz Biotechnology), Peroxisome proliferator-activated receptor gamma coactivator 1-alpha -PGC-1alpha 1:1,000 (#ab54481, Abcam Cambridge, Massachusetts), Peroxisome proliferator-activated receptor gamma coactivator 1-beta (PGCß) 1:1000 (#ab176328 Abcam), Glyceraldehyde-3-Phosphate Dehydrogenase (GAPDH) 1:5000 (#2118s, Cell signalling Technology, Danvers, Massachusetts) (12). Densitometry was performed using Image J version 1.39 (National Institutes of Health, Bethesda, Maryland).

FIGURE 1 Time Course for Systolic Blood Pressure

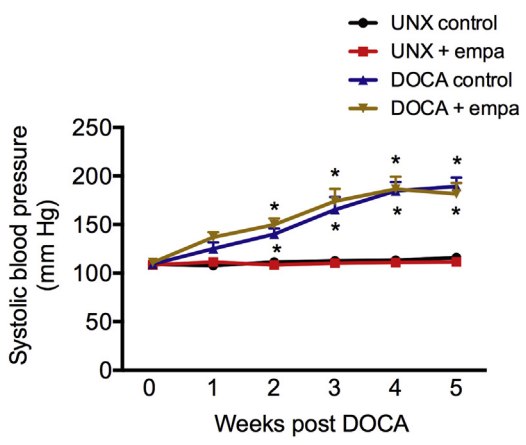

Time course for systolic blood pressure. n = 16 and 15 in deoxycorticosterone acetate (DOCA) control and empagliflozin (empa) groups, respectively. n = 7 to 8 in uninephrectomy (UNX) control and UNX empa groups. *p < 0.05 versus UNX + vehicle.

GENE EXPRESSION. The abundance of atrial natriuretic peptide (ANP), collagen 1/III, CD 36, PGC1α and β, Glut 1 and 4, hexokinase, pyruvate kinase, pyruvate dehydrogenase, carnitine palmitoyltransferase, uncoupling protein-3, nuclear respiratory factor-1, phosphoglucomutase-1, long-chain acyl-CoA dehydrogenase, GAPDH, pyruvate dehydrogenase E1-α subunit, ribosomal protein L13A (rRPL13a), and peroxisome proliferator–activated receptor-α were assessed by measuring their mRNA by quantitative real-time polymerase chain reaction in LV tissue stored at −80°C (10). In brief, SYBR Green (Life Technologies Corporation, Thermo Fisher, Waltham, Massachusetts) green-based measurement of gene expression was performed on the QuantStudio 7 Flex Real-Time PCR System (Applied Biosystems, Foster City, California) according to the manufacturer's instructions using the pre-designed sequence-specific primers from Integrated DNA Technologies (Coralville, Iowa). Data were analyzed using the Applied Biosystems Comparative Computer Tomography method. See Supplemental Table 1 for primers.

STATISTICAL ANALYSIS. Data are expressed as means ± SEM, unless otherwise specified. Between-group differences were analyzed by 2-way analysis of variance with Fisher's least significance difference post hoc test. Statistical analysis was performed using GraphPad Prism 6 for Mac OS X (GraphPad Software Inc., San Diego, California). A p value of <0.05 was regarded as statistically significant.

RESULTS

ANIMAL CHARACTERISTICS. Compared with UNX control rats, DOCA salt rats demonstrated significant reductions in both body weight and food intake, as well as hypertension, that developed 2 weeks after DOCA initiation (**Table 1, Figure 1**). Water intake and urine output also increased in parallel. Empagliflozin administration to DOCA salt animals further reduced body weight compared with control rats, without affecting food intake. DOCA salt animals displayed

increased heart weight and lung weight when indexed to tibial length, which was reduced with empagliflozin (Table 1). Both water intake and urine output were increased in proportion to each other in rats that had received empagliflozin in both control and DOCA salt settings.

LABORATORY PARAMETERS. Hematocrit and hemoglobin were lower in DOCA salt animals compared with control animals, and although these were not normalized to levels seen in control rats, hematocrit and hemoglobin were both substantially higher among DOCA salt rats that received empagliflozin (Table 2). Plasma sodium and 24-h urinary sodium excretion were increased in DOCA salt rats, although neither was affected by empagliflozin administration (Table 2).

Regardless of assignment to control or DOCA salt groups, animals that received empagliflozin showed substantial glucosuria, and, although still within the normoglycemic range, plasma glucose in DOCA salt rats was lower in those that received empagliflozin (Table 2). Urinary excretion of ß-OH-butyrate was higher in DOCA salt animals than that in control animals and did not differ

TABLE 2 Laboratory Parameters

	UNX + Control	UNX+ Empa	DOCA + Control	DOCA + Empa
Hct (%)	42.1 ± 0.7	41.0 ± 0.6	32.1 ± 1.8*	36.5 ± 0.8*†
Hb (g/l)	138.6 ± 1.9	136.6 ± 2.7	108.7 ± 4.6*	121.5 ± 3.6*†
U Na (mmol/l)	79.6 ± 12.0	44.6 ± 4.7	147.5 ± 16.0*	127.6 ± 13.4*
U Na (mmol/d)	2.03 ± 0.31	2.19 ± 0.33	22.3 ± 3.19*	26.6 ± 3.08*
P Na (mmol/l)	133.6 ± 0.7	135.6 ± 0.6	140.5 ± 0.7*	141.7 ± 0.5*
P Glu (mmol/l)	6.18 ± 0.19	5.91 ± 0.18	6.34 ± 0.13	5.71 ± 0.12*†
U Glu (mmol/l)	1.05 ± 0.58	60.0 ± 0.0*	0.9 ± 0.18	41.91 ± 4.38*†
U Glu (mmol/d)	0.03 ± 0.02	2.9 ± 0.31*	0.15 ± 0.04	8.15 ± 0.75*†
HbA_{1c} (%)	4.92 ± 0.18	4.66 ± 0.07	4.02 ± 0.02*	4.12 ± 0.10*
BHB (µmol/d)	1.65 ± 0.34	3.70 ± 0.41	13.43 ± 1.35*	15.18 ± 1.30*

Values are mean ± SEM. *p < 0.05 versus UNX + control group. †p < 0.05 versus DOCA + control group.
BHB = β-hydroxybutyrate; Glu = glucose; Hb = hemoglobin; Hct = hematocrit; Na = sodium; P = plasma; U = urine; other abbreviations as in Table 1.

FIGURE 2 Representative Echocardiograms

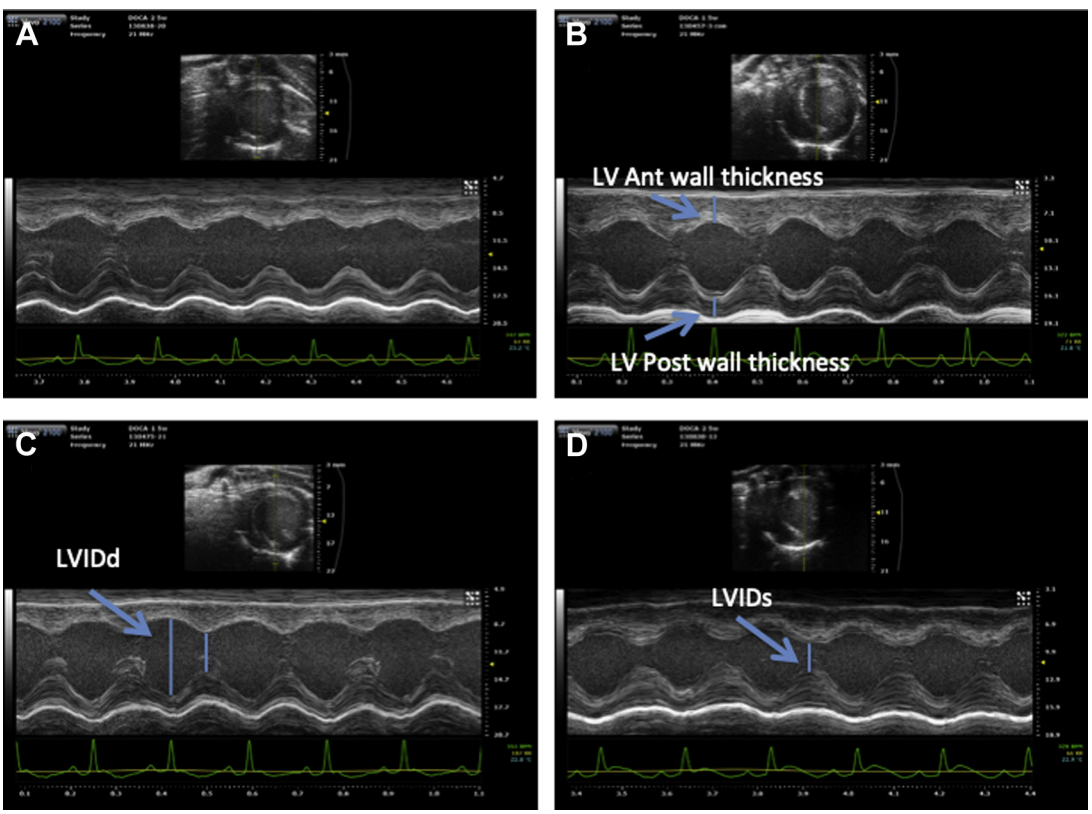

Representative echocardiograms (M-MODE) in **(A)** UNX + control, **(B)** UNX + empagliflozin, and **(C)** UNX + DOCA + control, and **(D)** UNX + DOCA + empa. Both left ventricular internal diameter systole (LVIDs) and wall thickness were reduced by empa in DOCA salt rats. *p < 0.05 versus UNX treated with vehicle. LVIDd = left ventricular internal diameter diastole; other abbreviations as Figure 1.

JACC: BASIC TO TRANSLATIONAL SCIENCE VOL. 4, NO. 1, 2019
FEBRUARY 2019:27–37

TABLE 3 Cardiac Function as Assessed by Echocardiography and Conductance Catheterization

	UNX + Control	UNX + Empa	DOCA + Control	DOCA + Empa
EF (%)	80 ± 2	80 ± 2	84 ± 2*	88 ± 1*
LVIDd (mm)	8.2 ± 0.3	8.1 ± 0.2	7.9 ± 0.2	7.3 ± 0.2*
LVIDs (mm)	4.0 ± 0.2	4.0 ± 0.2	3.5 ± 0.3	2.9 ± 0.2*†
LV mass corr. (mg)	1053 ± 57	975 ± 22	1520 ± 90*	1164 ± 51†
LVPWs (cm)	0.35 ± 0.01	0.35 ± 0.01	0.45 ± 0.02*	0.43 ± 0.01*
SBP (mm Hg)	116 ± 1	112 ± 2	188 ± 6*	182 ± 6*
Wall stress, σ (g/cm^2)	58 ± 5	61 ± 5	73 ± 6*	53 ± 4†
HR (beats/min)	370 ± 10	327 ± 10	334 ± 6*	334 ± 8*
EDP (mm Hg)	11 ± 1	12 ± 2	11 ± 1	11 ± 1
dP/dt_{max} (mm Hg/s)	6,557 ± 451	6,664 ± 324	6,092 ± 494	6,599 ± 377
dP/dt_{min} (mm Hg/s)	−7,596 ± 441	−7,387 ± 317	−5,580 ± 546*	−6,505 ± 548
EDPVR (mm Hg/μl)	0.017 ± 0.004	0.019 ± 0.003	0.024 ± 0.003	0.023 ± 0.002
Tau (ms)	11.5 ± 0.2	12.7 ± 0.7	15.1 ± 0.4*	13.5 ± 0.6*†

Values are mean ± SEM. n = 7 to 8 in UNX control and UNX Empa groups; n = 15 in DOCA control and Empa groups, respectively. *p < 0.05 versus UNX + vehicle. †p < 0.05 versus DOCA + vehicle.

dP/dt_{min} = maximal rate of pressure decline; EDP = end-diastolic pressure; EDPVR = end-diastolic pressure–volume relationship; EF = ejection fraction; HR = heart rate; LVIDd = left ventricular internal diameter in diastole; LVIDs = left ventricular internal dimension in systole; LV mass corr. = left ventricular mass corrected; LVPWs = left ventricular posterior wall in systole; SBP = systolic blood pressure; other abbreviations as in Table 1.

according to treatment assignment to empagliflozin or vehicle (Table 2).

ECHOCARDIOGRAPHY. DOCA salt rats demonstrated preserved EF with increased wall thickness and LV mass compared with control rats (Figure 2, Table 3).

FIGURE 3 Steady-State Pressure–Volume Loops

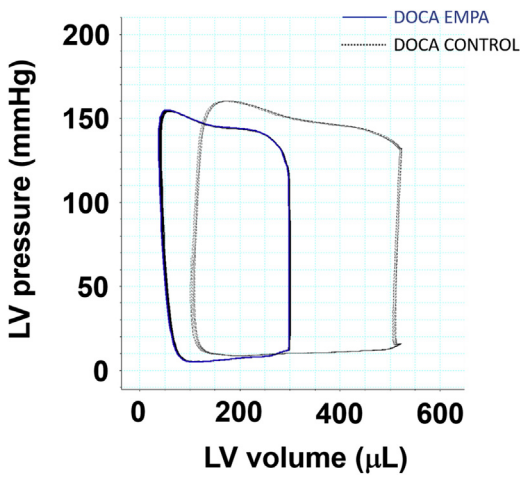

Empa-treated UNX + DOCA salt animals display a leftward shift with a reduction in end-diastolic volume **(blue curve)** compared with the UNX + DOCA salt control animals **(gray curve)**. Abbreviations as in Figures 1 and 2.

Empagliflozin therapy reduced LV end-systolic dimension, LV mass, and posterior wall thickness (Table 3).

CONDUCTANCE CATHETERIZATION. A high-fidelity LV pressure manometer was used to assess diastolic function. DOCA salt administration prolonged Tau and reduced dp/dt_{min}, which indicated impaired diastolic relaxation; these abnormalities were both ameliorated by empagliflozin (Table 3). Similarly, wall stress that was increased in DOCA salt rats was reduced with empagliflozin. In contrast, late diastolic relaxation, as assessed by the end-diastolic pressure–volume relationship, was not increased by DOCA salt and was unaffected by empagliflozin (Table 3, Figure 3).

HISTOLOGY. In keeping with the observed morphometric changes, DOCA salt rats demonstrated increased cardiomyocyte size compared with control rats, which was significantly reduced by empagliflozin therapy (Figure 4). Furthermore, DOCA salt treatment increased perivascular and interstitial LV fibrosis compared with control vehicle. Empagliflozin therapy did not affect the extent of LV fibrosis in either the perivascular or interstitial compartments.

MOLECULAR STUDIES. To assess the mechanism in which early active energy-dependent relaxation was improved with empagliflozin therapy, we assessed a range of proteins involved in calcium handling and the hypertrophic response. There was no significant change in SERCA2A content, nor in the total and/or phosphorylated phospholamban expression at either pSer16 or pThr17 sites. Furthermore, we assessed total and phosphorylated calcium and/or calmodulin-dependent protein kinase II to better elucidate the change in cardiomyocyte hypertrophy and identification of LV hypertrophy. There was no significant change seen with either DOCA or empagliflozin administration (Supplemental Figure 1).

DOCA salt treatment increased ANP, collagen 1, and III mRNA compared with control vehicle ($p < 0.05$). Empaglifozin treatment had no effect on collagen 1/III or ANP mRNA (Figure 5).

Because of the surprising absence of altered protein expression in key cardiac calcium handling proteins, we went on to assess whether the observed functional benefits were secondary to improved myocardial energetics. As a result, we performed RTq polymerase chain reaction on a panel of genes known to be involved in metabolism. UNX + DOCA had minimal effect on gene expression of the metabolic

FIGURE 4 Stained Sections

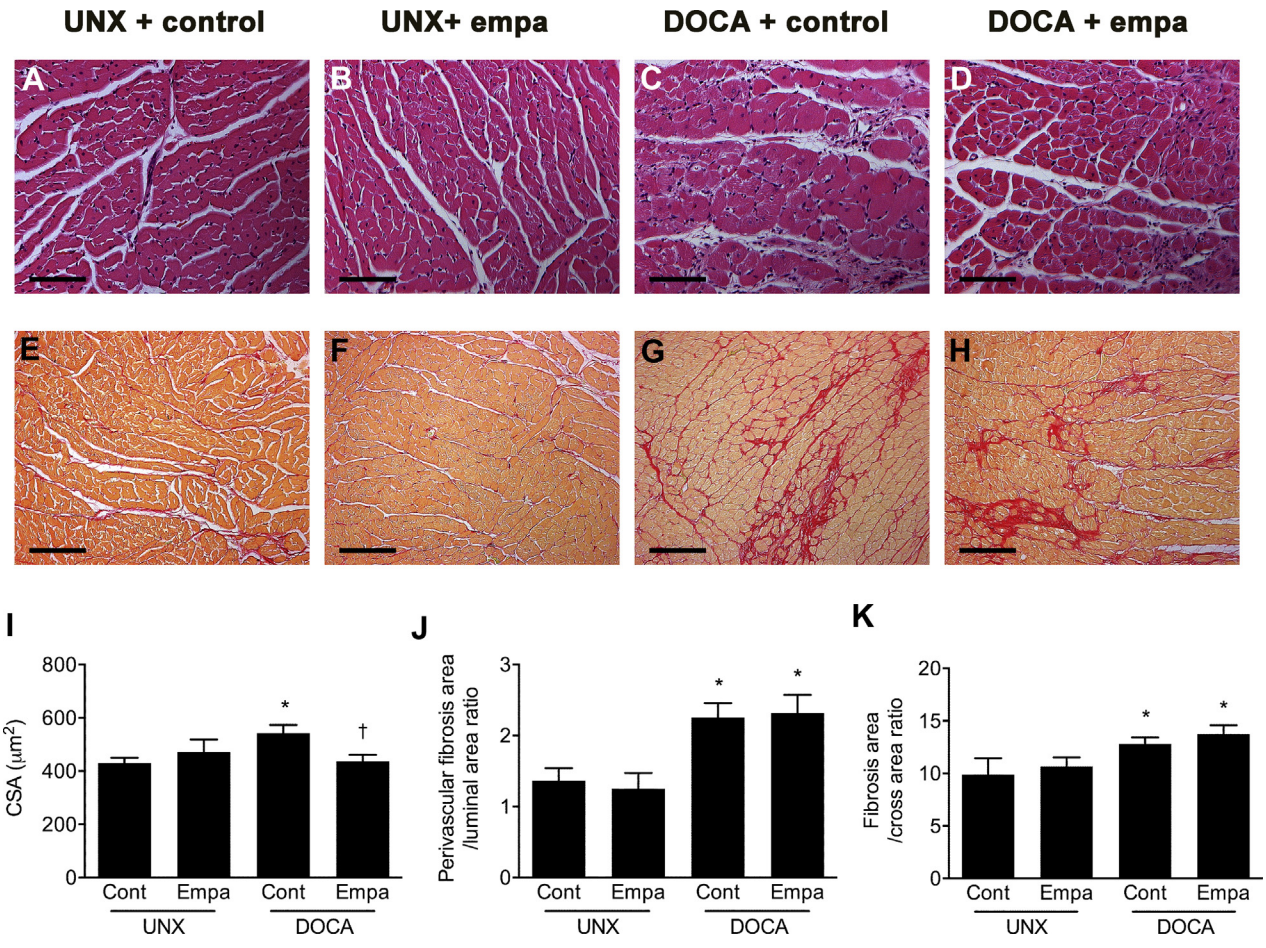

(A to D) Representative hematoxylin and eosin and **(E to H)** picrosirius red stained sections. Hearts of UNX + DOCA salt rats showed evidence of **(I)** myocyte hypertrophy, together with both **(J and K)** perivascular and interstitial fibrosis. Empa reduced cardiomyocyte size in UNX + DOCA animals but had no effect on either interstitial or perivascular fibrosis. n = 7 to 8 in UNX control and UNX empa groups; n = 16 and 15 in DOCA control and empa groups, respectively. *p < 0.05 treated with UNX + control. †p < 0.05 treated with UNX + DOCA + control. CSA = cross-sectional area; other abbreviations as in Figure 1.

genes presented (Supplemental Figure 2). However, there was a significant reduction in both PGC1α and fatty acid protein and/or CD36 expression that was improved by empagliflozin therapy ($p < 0.05$). The changes in mRNA expression were not accompanied by changes in protein abundance (Supplemental Figure 1).

DISCUSSION

Despite significant advances in the treatment of HFrEF, HFpEF lacks evidence-based therapies. We used a model of hypertension-induced HFpEF, the DOCA salt rat that demonstrates the cardinal manifestations of HFpEF. Without significantly affecting either blood pressure or glycemia, the SGLT2i, empagliflozin, reduced LV mass and attenuated the increased wall stress and impaired diastolic function that develop in this nondiabetic disease model.

Administration of the mineralocorticoid, DOCA, in combination with dietary salt loading increased cardiac afterload, which created pathological changes that are highly reminiscent of human hypertensive heart disease, with increased LV mass, cardiomyocyte hypertrophy, cardiac interstitial fibrosis, and impaired diastolic function (13). From a pathophysiological perspective, the requirement of the LV to approximate aortic pressure in systole increases intraventricular wall stress that can be further exacerbated by chamber dilatation. To mitigate an

FIGURE 5 Heart Collagen 1 and III, ANP mRNA Levels

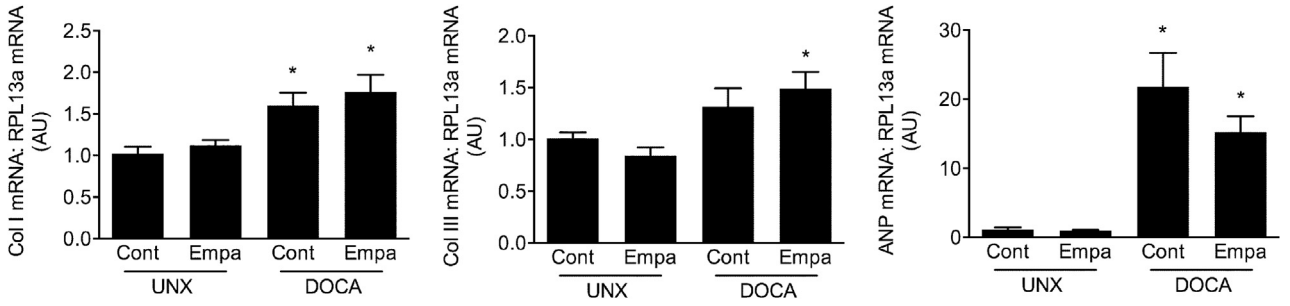

Hearts of DOCA salt rats showed evidence of atrial natriuretic peptide (ANP) activation, together with increased collagen I (Col I) and III mRNA. Empa had no effect on either ANP, or Col I or III mRNA. n = 8 for control (Cont) UNX; n = 7 for UNX empa; n = 14 for control DOCA; n = 13 for empa DOCA. *p < 0.05 compared to UNX animals treated with UNX + control. RPL13a = ribosomal protein L13A housekeeping gene; other abbreviations as in Figure 1.

increase in wall stress, there is an increase in wall thickness (i.e., hypertrophy) that allows the workload to be shared among a greater number of sarcomeric units. Although initially beneficial, the resultant changes in the pressure–volume relationship lead not only to cardiomyocyte hypertrophy but also to interstitial fibrosis, impaired relaxation, and ultimately HFpEF.

In contrast to vehicle-treated rats, the present study found that the administration of empagliflozin reduced LV mass and attenuated cardiomyocyte hypertrophy in conjunction with diminished wall stress and improved diastolic function. The attenuation in diastolic dysfunction was confined to the early, energy-dependent active phase of diastole as reflected by the shortening of the isovolumic relaxation constant (Tau) and a reduction in the minimum rate of ventricular pressure change (dP/dt_{min}). In contrast, dysfunction in the later energy-independent passive phase of diastole, as indicated by the end-diastolic pressure–volume relationship, was unaffected either by DOCA salt or by empagliflozin.

The previously noted changes in cardiac structure and function with empagliflozin provided a number of novel insights into the potential mode of action of the SGLT2 drug class in the HFpEF setting. As in humans with an excess of mineralocorticoid, the administration of DOCA in conjunction with a high salt diet leads to intravascular volume expansion, as indicated by reduced hematocrit. LV chamber volume, although not increased in this model, was nevertheless reduced by empagliflozin commensurate with an increase in hematocrit. Among animals on a normal diet that had not received DOCA, and in which intravascular volume was presumably normal, empagliflozin did not affect either hematocrit or chamber volume. These findings suggested that the beneficial effects of SGLT2 inhibition on the prevention of HF might be most marked when intravascular volume is increased.

The histopathological response to increased afterload included both cardiomyocyte hypertrophy and fibrosis with impairments in both the metabolically active, early component of diastole, together with the passive, later compliance-based phase. Unlike many other ostensibly cardioprotective agents that were examined in the DOCA salt model, which included angiotensin-converting enzyme inhibitors, angiotensin receptor blockers, mineralocorticoid receptor antagonists (14), dual vasopeptidase inhibitors (15), and endothelin antagonists (16), empagliflozin reduced hypertrophy and not fibrosis. Although interventions that reduce cardiac fibrosis also attenuated the abnormalities in passive diastolic compliance (6,17,18), this component of diastolic function was not abnormal in DOCA salt rats in the present study.

To elucidate the molecular mechanisms behind the improved diastolic function and early active relaxation, we performed Western blot analyses of a range of proteins involved in cardiac calcium handling. We observed minimal changes in proteins involved in relaxation or the hypertrophic response (Supplemental Figure 1). The lack of change led us to investigate whether the improved cardiac diastolic

function was secondary to improved myocardial energetics induced by empagliflozin therapy. We used RTq polymerase chain reaction to assess a wide range of genes known to be involved in fatty acid transport, fat, and glucose oxidation, as well as mitochondrial biogenesis (Supplemental Figure 2) (19). Much to our surprise, these results demonstrated minimal change in gene expression. We observed downregulated expression of uncoupling protein 3, PGC1α, pyruvate kinase, and CD36/fatty acid protein only in DOCA salt UNX animals. Empagliflozin therapy improved PGC1α gene expression in DOCA UNX animals, but we observed no change in protein content. Although at first these findings appeared incongruous to the functional improvements seen, they were in keeping with data from a wide body of investigators who demonstrated that most of benefits in rodents occurred from the hemodynamic effects and hemoconcentration, and not from altered energetics as a result of ketone metabolism (20,21).

To date, a wide range of hypotheses have been put forward to explain the reduction in HF hospitalization seen in the cardiovascular trials with SGLT2s, EMPA-REG Outcome trial (Empagliflozin, Cardiovascular Outcomes, and Mortality in Type 2 Diabetes trial) and CANVAS (CANagliflozin cardioVascular Assessment Study) trial, using 2 different SGLTs, empagliflozin and canagliflozin, respectively, and a third trial that will report shortly (3,4). Among these theories, considerable interest has focused on the proposal by Ferranini and Mayoux (22) that these salutary cardiac effects of SGLT2 inhibitors may be dependent on augmented ketone body formation and increased hematocrit. As elaborated on in their seminal paper, the investigators speculated that the reduction in HF with empagliflozin reflected the improved cardiac energetics that follow augmented ß-hydroxy-butyrate production coupled with enhanced oxygen delivery to the myocardium as a consequence of hemoconcentration. In the present study, conducted in the nondiabetic setting, we did not observe any differences in ß-hydroxy-butyrate between rats that had received either empagliflozin or vehicle. We did find an increase in hematocrit and improved cardiac function in animals treated with empagliflozin, which was consistent with the results of the recently published mediation analysis (20). Whether the relationship between hematocrit and cardiovascular outcome as seen in the EMPA-REG Outcome study might be a consequence of volume contraction, improved oxygen delivery, or both, could not be discerned from the present experimental study.

STUDY LIMITATIONS. Our study was not without limitations. First, empagliflozin therapy was commenced soon after DOCA was first administered. As such, further studies would be required to assess whether late treatment might also reverse the structural and functional manifestations of established HFpEF. Second, although DOCA salt is a well-validated model of HFpEF (23-25), it is only 1 example of the disorder. However, work by other investigators in an alternate model of HEpEF (pressure overload) demonstrated similar findings with improvement in diastolic function in response to SGLT2 inhibition (26). Similar to our work, the exact molecular mechanism by which this occurred remains elusive and requires further investigation. Finally, although we did not find any statistical differences in systolic blood pressure, as shown in **Figure 1**, levels were numerically slightly lower in DOCA salt animals that received empagliflozin compared with those that did not throughout much of the study.

CONCLUSIONS

Empagliflozin therapy reduced lung weight, improved LV mass, and ameliorated diastolic dysfunction in a rodent model of HFpEF. Potential pathophysiological mechanisms that underlie these salutary changes are likely multifactorial. Such factors include diminished pre-load and possibly afterload that reduce myocardial oxygen demand, along with an elevated hematocrit that proves increased oxygen delivery.

ADDRESS FOR CORRESPONDENCE: Dr. Kim A. Connelly, Keenan Research Centre, Li Ka Shang Knowledge Institute, St. Michael's Hospital, 61 Queen Street East, Toronto, Ontario M5C 2T2, Canada. E-mail: Connellyk@smh.ca.

JACC: BASIC TO TRANSLATIONAL SCIENCE VOL. 4, NO. 1, 2019
FEBRUARY 2019:27–37

PERSPECTIVES

COMPETENCY IN MEDICAL KNOWLEDGE: Despite 3 large trials demonstrating that SGLT2is reduced HF hospitalizations in patients with type 2 diabetes, the mechanisms underlying the observed benefit remain unclear. Currently, changes in hematocrit, pre-load, and afterload, together with altered myocardial energetics and metabolism, remain likely factors. We assessed the impact of empagliflozin on cardiac function structure in the UNX DOCA salt-sensitive rat, which was a nondiabetic experimental model of HFpEF.

TRANSLATIONAL OUTLOOK: Our study demonstrated that UNX male Sprague-Dawley rats that received DOCA in conjunction with 1% sodium chloride in drinking water (DOCA salt) developed hypertension and HFpEF in the absence of diabetes. Without significantly lowering blood pressure, empagliflozin reduced LV mass and ameliorated myocyte hypertrophy, which normalized LV wall stress and improved diastolic function. Importantly, these changes occurred in the absence of alterations in key calcium handling and hypertrophy signalling pathways, as well as key molecular markers of metabolism. These finding suggested that the impact of empagliflozin occurred primarily through altered hemodynamic effects, which provides a strong rationale for clinical studies in both HFrEF and HFpEF, regardless of diabetes status.

REFERENCES

1. Yeung DF, Boom NK, Guo H, Lee DS, Schultz SE, Tu JV. Trends in the incidence and outcomes of heart failure in Ontario, Canada: 1997 to 2007. CMAJ 2012;184:E765–73.

2. Bhatia RS, Tu JV, Lee DS, et al. Outcome of heart failure with preserved ejection fraction in a population-based study. N Engl J Med 2006;355:260–9.

3. Zinman B, Wanner C, Lachin JM, et al. Empagliflozin, cardiovascular outcomes, and mortality in type 2 diabetes. N Engl J Med 2015;373:2117–28.

4. Neal B, Perkovic V, Mahaffey KW, et al. Canagliflozin and cardiovascular and renal events in type 2 diabetes. N Engl J Med 2017;377:644–57.

5. Viel EC, Benkirane K, Javeshghani D, Touyz RM, Schiffrin EL. Xanthine oxidase and mitochondria contribute to vascular superoxide anion generation in DOCA-salt hypertensive rats. Am J Physiol Heart Circ Physiol 2008;295:H281–8.

6. Connelly KA, Kelly DJ, Zhang Y, et al. Inhibition of protein kinase C-beta by ruboxistaurin preserves cardiac function and reduces extracellular matrix production in diabetic cardiomyopathy. Circ Heart Fail 2009;2:129–37.

7. Bugyei-Twum A, Abadeh A, Thai K, et al. Suppression of NLRP3 inflammasome activation ameliorates chronic kidney disease-induced cardiac fibrosis and diastolic dysfunction. Sci Rep 2016;6:39551.

8. Connelly KA, Advani A, Kim S, et al. The cardiac (pro)renin receptor is primarily expressed in myocyte transverse tubules and is increased in experimental diabetic cardiomyopathy. J Hypertens 2011;29:1175–84.

9. Dong H, Mosca H, Gao E, Akins RE, Gidding SS, Tsuda T. Integrated wall stress: a new methodological approach to assess ventricular workload and myocardial contractile reserve. J Transl Med 2013;11:183.

10. Connelly KA, Kelly DJ, Zhang Y, et al. Functional, structural and molecular aspects of diastolic heart failure in the diabetic (mRen-2)27 rat. Cardiovasc Res 2007;76:280–91.

11. Civitarese RA, Talior-Volodarsky I, Desjardins JF, et al. The alpha11 integrin mediates fibroblast-extracellular matrix-cardiomyocyte interactions in health and disease. Am J Physiol Heart Circ Physiol 2016;311:H96–106.

12. Batchu SN, Thieme K, Zadeh FH, et al. The dipeptidyl peptidase-4 substrate CXCL12 has opposing cardiac effects in young mice and aged diabetic mice mediated by Ca(2+) flux and phosphoinositide 3-kinase gamma. Diabetes 2018;67:2443–55.

13. Iyer A, Chan V, Brown L. The DOCA-salt hypertensive rat as a model of cardiovascular oxidative and inflammatory stress. Curr Cardiol Rev 2010;6:291–7.

14. Brown L, Duce B, Miric G, Sernia C. Reversal of cardiac fibrosis in deoxycorticosterone acetate-salt hypertensive rats by inhibition of the renin-angiotensin system. J Am Soc Nephrol 1999;10 Suppl 11:S143–8.

15. Pu Q, Amiri F, Gannon P, Schiffrin EL. Dual angiotensin-converting enzyme/neutral endopeptidase inhibition on cardiac and renal fibrosis and inflammation in DOCA-salt hypertensive rats. J Hypertens 2005;23:401–9.

16. Ammarguellat F, Larouche I, Schiffrin EL. Myocardial fibrosis in DOCA-salt hypertensive rats: effect of endothelin ET(A) receptor antagonism. Circulation 2001;103:319–24.

17. Yuen DA, Connelly KA, Advani A, et al. Culture-modified bone marrow cells attenuate cardiac and renal injury in a chronic kidney disease rat model via a novel antifibrotic mechanism. PLoS One 2010;5:e9543.

18. Zhang Y, Connelly KA, Thai K, et al. Sirtuin 1 activation reduces transforming growth factor-beta1-induced fibrogenesis and affords organ protection in a model of progressive, experimental kidney and associated cardiac disease. Am J Pathol 2017;187:80–90.

19. Kato T, Niizuma S, Inuzuka Y, et al. Analysis of metabolic remodeling in compensated left ventricular hypertrophy and heart failure. Circ Heart Fail 2010;3:420–30.

20. Inzucchi SE, Zinman B, Fitchett D, et al. How does empagliflozin reduce cardiovascular mortality? Insights from a mediation analysis of the EMPA-REG OUTCOME trial. Diabetes Care 2018;41:356–63.

21. Lopaschuk GD, Verma S. Empagliflozin's fuel hypothesis: not so soon. Cell Metab 2016;24:200–2.

22. Ferrannini E, Mark M, Mayoux E. CV Protection in the EMPA-REG OUTCOME trial: a "thrifty substrate" hypothesis. Diabetes Care 2016;39:1108–14.

23. Ogata T, Miyauchi T, Sakai S, Takanashi M, Irukayama-Tomobe Y, Yamaguchi I. Myocardial fibrosis and diastolic dysfunction in deoxycorticosterone acetate-salt hypertensive rats

is ameliorated by the peroxisome proliferator-activated receptor-alpha activator fenofibrate, partly by suppressing inflammatory responses associated with the nuclear factor-kappa-B pathway. J Am Coll Cardiol 2004;43:1481–8.

24. Schwarzl M, Hamdani N, Seiler S, et al. A porcine model of hypertensive cardiomyopathy: implications for heart failure with preserved ejection fraction. Am J Physiol Heart Circ Physiol 2015;309:H1407–18.

25. Allan A, Fenning A, Levick S, Hoey A, Brown L. Reversal of cardiac dysfunction by selective ET-A receptor antagonism. Br J Pharmacol 2005;146:846–53.

26. Byrne N, Parajuli N, Levasseu RJ, et al. Empagliflozin prevents worsening of cardiac function in an experimental model of pressure overload-induced heart failure. J Am Coll Cardiol Basic Trans Science 2017;2:347–54.

KEY WORDS diastole, heart failure with preserved ejection fraction, sodium-glucose–linked co-transporter-2 inhibitor, systole

APPENDIX For supplemental tables and figures, please see the online version of this paper.